Effective elastic constants and phonon spectrum in metallic Ta/Al quasiperiodic superlattices

Hua Xia
Chinese Center of Advanced Science and Technology (World Laboratory), P. O. Box 8730, Beijing 100080, People's Republic of China and National Laboratory of Solid State Microstructures, Nanjing University, Nanjing 210008, People's Republic of China

X. K. Zhang, An Hu, S. S. Jiang, R. W. Peng, Wei Zhang, and Duan Feng
National Laboratory of Solid State Microstructures, Nanjing University, Nanjing 210008, People's Republic of China

G. Carlotti, D. Fioretto, G. Socino, and L. Verdini
Laboratorio di Scattering Brillouin, Dipartimento di Fisica, Universitá di Perugia, I-06100 Perugia, Italy
(Received 8 September 1992)

The propagation of acoustic waves in superlattices is investigated within the effective-medium model generalized to the quasiperiodic structure. The effective elastic constants are analytically obtained in closed form for superlattices with hexagonal symmetry. These results are used to interpret the observed low-frequency phonon spectra from Ta/Al superlattices with quasiperiodic Fibonacci ordering and the elastic constants c_{11} and c_{44} for the superlattices are determined by fitting the data with an acoustic model of supported hexagonal films. The relative Brillouin cross section is found to be accurately represented by a pure ripple effect without photoelastic contribution. We show that the measured and calculated c_{11} demonstrates a reasonable agreement, but an appreciable discrepancy of $\sim 20\%$ for c_{44} is found. The implication of these results is discussed in detail.

I. INTRODUCTION

The structural and vibrational properties of one-dimensional (1D) quasiperiodic Fibonacci superlattices (QPFSL's) have been the subject of a large number of both theoretical and experimental investigations. Such artificially structured superlattices have shown rich and interesting spectral behavior relevant to 1D quasicrystals. We note, however, that most of the previous work has concentrated on the study of higher-frequency phonons from Fibonacci-modulated semiconductor superlattices via Raman scattering.[1-6] The obtained off-resonance phonon spectra show that the allowed phonon scattering forms a self-similar Cantor set and is dominated by doublets resembling folded acoustic modes in periodic superlattices.

These phonon spectra are actually determined by the superlattice sound velocity propagating along the growth direction. This velocity, determined by the effective elastic constant c_{33} of the QPFSL's, is usually taken as the spatial average of the sound velocity in each constituent layer.[3] However, even for GaAs/$Ga_{1-x}Al_xAs$ QPFSL's, this averaging procedure is incorrect in practice.[7] Although such a treatment does not significantly affect the explanation of hierarchical splitting of phonon spectra, the discrepancy between the experimental data and the theoretical prediction should not be ignored. To calculate accurately the phonon spectra and their dependence on the structural parameters, a more general theory and relevant Brillouin measurement for the effective elastic constants of the QPFSL's thus become necessary.

The investigation of such effective constants is usually related to the observation of a low-frequency phonon with a frequency shift less than 1 cm^{-1}. In this frequency regime, the acoustic modes have a wavelike feature and behave just like their counterparts in a supported film or a semi-infinite material. Observation of these acoustic modes and their dependence on the structural parameters thus provide direct insight into the elastic properties of a superlattice. From a different point of view, however, the study of such effective properties in quasiperiodic structures is also of major importance to surface-wave devices, optical and acoustic elements, and ultrasonic application in medicine.

Brillouin scattering is an ideal technique for the characterization of such thin-film materials since the incident laser light can be focused to dimensions of the order of those of the multilayers. Thus, it has been proved to be a powerful tool for gaining substantial insight into the physics of these multilayers by use of the high-contrast tandem Fabry-Pérot interferometer.[8] By observing the surface acoustic modes, one can determine the elastic constants and therefore the vibrational properties. In this paper we shall study both theoretically and experimentally the effective elastic properties through wave propagation in quasiperiodic structures. In particular, we report on our observation of the low-frequency phonon spectra from metallic Ta/Al QPFSL's by means of Brillouin scattering. The Ta/Al system has been selected not only for its practical importance as an optical element for soft x rays, but also for its model character and anomalous mechanical behavior. We develop a Fourier-transform technique suitable for the calculation of effective elastic properties in a superlattice with quasiperiodic sequence. We shall show how the elastic constants of the QPFSL's are determined from the measured phonon spectrum and theoretical analysis.

The outline of this paper is as follows. In the next section the experimental details are outlined. The theoretical formalism is described in Sec. III according to the effective-medium model. Specifically, the effective elastic constants in quasiperiodic system with hexagonal symme-

try are derived by using analytic expressions within a formal theory generalizing that of Grimsditch and Nizzoli for the elastic constants of periodic structures. Section IV shows how the elastic constants of the Ta/Al quasiperiodic superlattice are calculated, and presents a comparison of the experimental results with such calculations as well as with the Brillouin cross section. Furthermore, the effect of the presence of a diffuse interface on the elastic properties is discussed, and it seems capable of qualitatively accounting for the enhanced shear modulus found experimentally. In Sec. V, a summary and conclusions are given.

II. EXPERIMENTAL DETAILS

The samples used in this study were made up of alternating layers of Al and Ta, deposited by magnetron sputtering techniques onto a glass substrate, as described elsewhere.[9] Detailed prescriptions for forming a Fibonacci superlattice from two structural elements A and B can be found in Ref. 1. For the Ta/Al samples we studied here, each of the two basic elements A and B are subdivided into an Al layer of thickness d_1^A and d_1^B, plus a Ta layer of thickness d_2. Calculations based on the growth rate result in the following estimates of the layer thickness: $d_A = 46.6$ Å and $d_B = 29.6$ Å; the associated quasiperiodicity is $d = \tau d_A + d_B = 105$ Å, where $\tau = (1+\sqrt{5})/2$. 13-generation superlattices were prepared according to the Fibonacci sequence, for a total thickness of $h = 1.52$ μm.

Structural characterization of the samples was accomplished with standard Cu $K\alpha$ x-ray-diffraction equipment. We find from this measurement that aluminum and tantalum, respectively, grow with their (111) and (110) planes nearly parallel to the substrate surface. Meanwhile, crystallites in the samples are oriented randomly and uniformly about the axis normal to the surface. In a recent publication by three of us,[10] measurements at both low and high angles demonstrated that the angular position of the superlattice peaks satisfies the wave-vector relationship of $k_{p,n} = k_{p-1,n} + k_{p+1,n}$, where $k_{p,n} = 2\pi n \tau^p d^{-1}$, n and p being arbitrary integers. From the structural point of view, a high-quality metallic quasiperiodic superlattice has been obtained.

Brillouin spectra were obtained in air at room temperature with ~100 mW of p-polarized 5145-Å radiation. The scattered light was analyzed by a high-resolution six-pass tandem Fabry-Pérot interferometer in a backscattering geometry. In this case, the wave vector q of surface phonons coming into the scattering process is fixed by the conservation of momentum $q = 2k \sin\theta$, where k is the optical wave number and θ is the angle of incidence of light. To prevent detector saturation, an acousto-optic modulator attenuates the laser light while scanning through the bright elastically scattered light. Measurements have been taken with a data-acquisition time of about two hours.

III. EFFECTIVE ELASTIC CONSTANTS IN QPFSL's

In contrast to semiconductor superlattices (GaAs/AlAs, Si/Ge_xSi_{1-x}) where the photoelastic process dominates, the scattering activity of acoustic waves in most metallic superlattices is mainly due to the surface ripple effect, the process by which light couples to thermal fluctuations in matter. Thermally excited acoustic waves, which corrugate the nominally planar surface, produce a small cross section for inelastic optical scattering.[11] The component of momentum parallel to the surface is conserved in this process and the shift in frequency of the scattered light depends mainly on the effective elastic constants of the sample, in addition to the geometry of the incident and scattered beams.

For hexagonal metallic superlattices on a substrate, the Rayleigh wave (RW) is always observed, but the higher-order surface Sezawa modes exist only in the sound-velocity regime bounded by the transverse sound velocities of the film (v_t^f) and the substrate (v_t^s) for the case $v_t^f < v_t^s$. All of these modes consist of shear vertical and longitudinal polarized partial waves whose field components propagate parallel to the surface and decay exponentially with distance into the substrate. The effective elastic constants, except c_{12}, can thus be experimentally determined from the frequency shift and velocity dispersion of such modes.

Theoretically, to obtain such effective elastic constants, one must formulate the more general problems of acoustic-wave propagation in a QPFSL with arbitrary symmetry. One limit of the wave propagation corresponds to the case when the acoustic wavelength is large compared with the quasiperiodicity. Therefore, the effective fields of strain and stress for quasiperiodic combinations of these two basic elements can be expressed as a function of these fields in the individual elements. For an infinitely extended QPFSL, a schematic picture of this system is shown in Fig. 1. We denote the effective elastic, stress, and strain tensors in these two basic elements by $[C^\alpha]$, $[\sigma^\alpha]$, and $[\epsilon^\alpha]$ for $\alpha = A,B$, while those of the whole structure without superscripts refer to the effective properties of the QPFSL's. General expressions of the strain and stress fields can be obtained by the Fourier transformation:

$$\sigma_{ij}^{\mathrm{QPFSL}} = \left[\frac{\tau d_A}{d}\sigma_{ij}^A + \frac{d_B}{d}\sigma_{ij}^B\right]\delta(k) + \frac{d}{\pi^2 d_A}(\sigma_{ij}^A - \sigma_{ij}^B)\sum_{p\neq 0} S(k_p)\delta(k-k_p)\,, \quad \text{with } (i,j) = (1,1),(1,2),(2,2)\,, \tag{1}$$

$$\epsilon_{ij}^{\mathrm{QPFSL}} = \left[\frac{\tau d_A}{d}\epsilon_{ij}^A + \frac{d_B}{d}\epsilon_{ij}^B\right]\delta(k) + \frac{d}{\pi^2 d_A}(\epsilon_{ij}^A - \epsilon_{ij}^B)\sum_{p\neq 0} S(k_p)\delta(k-k_p)\,, \quad \text{with } (i,j) = (1,3)(2,3),(3,3)\,, \tag{2}$$

where $|S(k_p)| = |\sin(\pi d_2 \tau^p/d)\sin(\pi d_A \tau^{2-p}/d)|$.

In general cases, the local displacement from equilibrium for the acoustic phonon can be approximated by simple plane waves with an effective sound velocity and the local stress component is proportional to the relevant acoustic impedance.[12,13] In addition, the effect of the

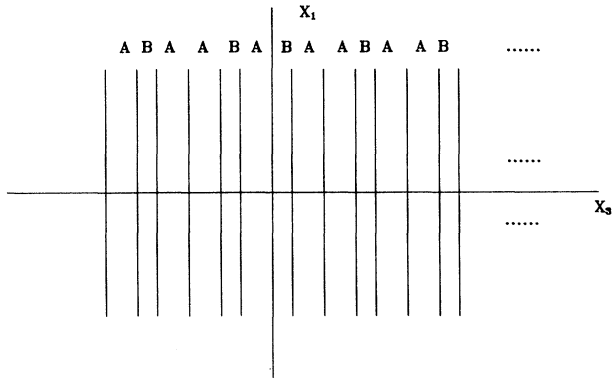

FIG. 1. Infinitely extended quasiperiodic layered structure $ABAABABAABAAB\cdots$. We consider the acoustic waves propagating both parallel and perpendicular to the superlattice axis, where the x_3 axis is chosen along the normal direction and x_1 parallel to the surface.

acoustic-impedance mismatch on the wave propagation may be important due to acoustic coupling between plane waves whose wave vectors differ by a reciprocal-lattice-vector value. Only when the Fourier component of such an effect is negligible and when all of the waves are decoupled will this allow us to ignore the contribution from high-order terms of the Fourier series.[14,15] Hence Eqs. (1) and (2) reduce to the effective-medium model. According to this model, the effective elastic tensor can be derived as follows.

The local stress and strain components must be continuous at the interfaces between adjacent layers. Specifically, these conditions are given by

$$\epsilon_{ij}^{\mathrm{QPFSL}}=\epsilon_{ij}^{A}=\epsilon_{ij}^{B} \quad \text{for } (i,j)=(1,1),(1,2),(2,2)\ , \tag{3}$$

$$\sigma_{ij}^{\mathrm{QPFSL}}=\sigma_{ij}^{A}=\sigma_{ij}^{B} \quad \text{for } (i,j)=(1,3),(2,3),(3,3)\ . \tag{4}$$

Correspondingly, the effective mass density can be reasonably taken to be

$$\rho=\frac{\tau d_A}{d}\rho_A+\frac{d_B}{d}\rho_B\ . \tag{5}$$

Generalized expressions for the effective constants of a quasiperiodic superlattice can be obtained by using a similar procedure as has been developed in Refs. 16–19 for periodic superlattices. Thus, we are able to derive the following effective elastic-stiffness tensor of quasiperiodic superlattices as

$$[C^{\mathrm{QPFSL}}]=\left[\frac{\tau d_A}{d}[C^A][U^A]^{-1}+\frac{d_B}{d}[C^B][U^B]^{-1}\right]\times\left[\frac{\tau d_A}{d}[U^A]^{-1}+\frac{d_B}{d}[U^B]^{-1}\right]^{-1}\ , \tag{6}$$

where $[C^j]$ are elastic-stiffness tensors in the A and B elements, and $[U^j]^{-1}$ is the inverse of the 6×6 matrix $[U^j]$, defined by

$$[U^j]=\begin{bmatrix} 1 & 0 & 0 & 0 & 0 & 0 \\ 0 & 1 & 0 & 0 & 0 & 0 \\ c_{13}^j & c_{23}^j & c_{33}^j & c_{34}^j & c_{35}^j & c_{36}^j \\ c_{14}^j & c_{24}^j & c_{34}^j & c_{44}^j & c_{45}^j & c_{46}^j \\ c_{15}^j & c_{25}^j & c_{35}^j & c_{45}^j & c_{55}^j & c_{56}^j \\ 0 & 0 & 0 & 0 & 0 & 1 \end{bmatrix}\ ,$$

for $j=A$ and B .

According to Eq. (6), the effective elastic constants can always be evaluated at least numerically. To the advantage of both experimental investigation and theoretical analysis for metallic superlattices, we only present such constants of quasiperiodic superlattices composed of basic elements of hexagonal symmetry with a symmetry axis normal to the surface. The analytical solutions are

$$\frac{d}{C_{33}^{\mathrm{QPFSL}}}=\frac{\tau d_A}{C_{33}^A}+\frac{d_B}{C_{33}^B}\ ,\quad \frac{d}{C_{44}^{\mathrm{QPFSL}}}=\frac{\tau d_A}{C_{44}^A}+\frac{d_B}{C_{44}^B}\ , \tag{7}$$

$$\frac{dC_{13}^{\mathrm{QPFSL}}}{C_{33}^{\mathrm{QPFSL}}}=\frac{\tau d_A C_{13}^A}{C_{33}^A}+\frac{d_B C_{13}^B}{C_{33}^B}\ , \tag{8}$$

$$C_{11}^{\mathrm{QPFSL}}-\frac{C_{13}^{2\,\mathrm{QPFSL}}}{C_{33}^{\mathrm{QPFSL}}}=\frac{\tau d_A}{d}\left[C_{11}^A-\frac{C_{13}^{2\,A}}{C_{33}^A}\right]+\frac{d_B}{d}\left[C_{11}^B-\frac{C_{13}^{2\,B}}{C_{33}^B}\right]\ , \tag{9}$$

and

$$C_{66}^{\mathrm{QPFSL}}=\frac{\tau d_A}{d}C_{66}^A+\frac{d_B}{d}C_{66}^B\ . \tag{10}$$

The above derivation is straightforward, though somewhat tedious. These constants are clearly coupled; once the key constant C_{33} is solved, the other constants are readily obtained. We note that the expressions of these effective constants represent no remarkable changes when compared with those of periodic superlattices if one defines $f_A=\tau d_A/d$ and $f_B=d_B/d$.[19] This property, implying periodicity on a logarithmic scale, reflects the self-similarity of the Fibonacci sequence. On the other hand, this also coincides with the fact that the long-wavelength acoustic modes are insensitive to microscopic detail when the wavelength of such modes is comparable to, or larger than, the quasiperiodicity or periodicity of a superlattice. Therefore quasiperiodic superlattices may be like an effective homogeneous medium whose effective constants are related only to those of its constituent layers. But the differences between quasiperiodic and periodic results may still be striking if the acoustic-impedance mismatch is appreciable.[7,14,20] In this case, the contribution of the higher-frequency acoustic phonons in the so-called reduced Brillouin zone to the elastic constants should be taken into account.

IV. RESULTS AND DISCUSSION

Brillouin spectra for two quasiperiodic superlattices were recorded for which all the sample parameters are nearly identical. Each spectrum consists of one sharp peak and an extended shoulder roughly symmetric about zero-frequency shift. Typical spectra from Ta/Al QPFSL's grown on glass, obtained for two incidence angles, are presented in Fig. 2. The pronounced peak at about 8 GHz is due to the Rayleigh wave propagating parallel to the surface. Its phase velocity is determined by $v_R=\omega/q$, where ω is the measured frequency shift obtained through the average of the Stokes and anti-Stokes shifts. Measurement reproducibility indicates that the uncertainty in the sound velocity v_R is about 1%.

At higher frequencies we see a shoulder up to about 19 GHz, originating from the contribution of bulk-acoustic modes. This is usually observed in Brillouin spectra from thick metallic films, since as the thickness of the film becomes greater than the phonon wavelength, the number of allowed discrete acoustic modes increases up to a continuum of modes. In this continuous part, one can recognize a minimum located at the frequency of longitudinal acoustic phonons,[8] as denoted by the insets, where the fitted solid curves in the insets are only a least-squares fit to the experimental data. Since the frequency location of this minimum and the velocity of the Rayleigh wave depend essentially on c_{11} and c_{44} in the present case, we have therefore achieved a selective determination of both $c_{11}=167\pm7$ and $c_{44}=38\pm0.5$ GPa, respectively.

To compare these experimental values with those predicted, we have performed the following calculations. Since our Ta/Al samples are polycrystalline and the crystallites are oriented randomly and uniformly about the axis normal to the surface, the elastic constants of the film can be estimated based on the bulk properties of the single-crystal constituent metals, by taking the Voigt (Reuss) estimate[21] into account. Starting from the bulk elastic constants of Al and Ta, the elastic constants of polycrystalline Al(111) and Ta(110) were obtained, as listed in Table I.

Since a quasiperiodic Fibonacci lattice can be regarded as a superposition of two incommensurate periods which are, respectively, proportional to the Fibonacci numbers F_j and F_{j-1} defined iteratively by the recursion $F_j=F_{j-1}+F_{j-2}$ for $j\geq2$, with $F_0=0$ and $F_1=1$, for a quasiperiodic superlattice of higher generation, the

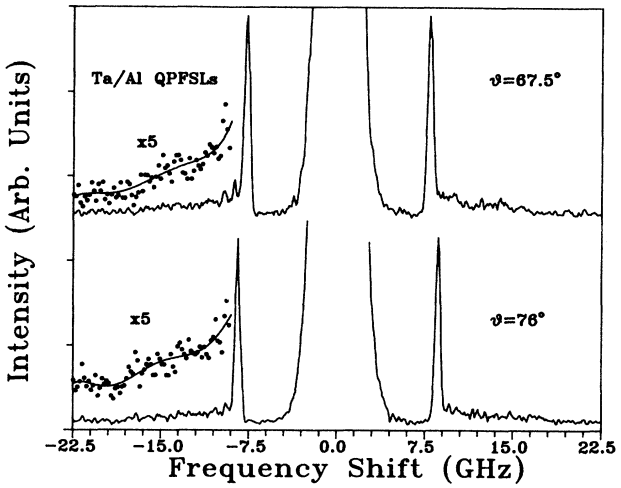

FIG. 2. Typical Brillouin spectra from a Ta/Al quasiperiodic superlattice with quasiperiodicity $d=105$ Å and total thickness 1.52 μm. The pronounced peaks are due to the Rayleigh acoustic wave propagating along surface. The solid curves in the insets are only a least-squares fit to the experimental data.

period ratio F_j/F_{j-1} of two sublattices approaches the irrational golden mean τ. Consequently, the effective constants $c_{ij}^{\alpha}(\alpha=A,B)$ of the elements A and B can be calculated in a way similar to that of a periodic superlattice.[16–19]

The effective elastic constants of Ta/Al QPFSL's based on our structural parameters and Eqs. (7)–(10) have also been listed in Table I. One finds that the measured c_{11} is only ~3% higher than the value calculated. However, the measured shear constant c_{44} is found to be about 20% higher than the expected value. Since the absolute elastic constants obtained from the Brillouin measurements, in the limit of thick films, are at best only accurate to ~5%, the measured c_{11} may thus be considered comparable to that calculated by Eq. (9) within experimental error.

To explain the discrepancy between the measured and evaluated shear modulus, we first considered the choice of bulk constants from the single-crystal values, especially for the shear modulus; but the variation in amplitude of c_{44} is far less than 20%. Experimentally, the Brillouin

TABLE I. Effective elastic constants and mass density calculated by use of the effective-medium model. The corresponding phase velocity of the Rayleigh wave, for each material, is shown in the last column. For comparison, the last row shows the values measured experimentally.

	C_{11}	C_{33}	C_{44}	C_{12} GPa	C_{13}	ρ g/cm^3	v_R m/s
Al(111)	112.8	115.0	24.8	60.2	58.5	2.70	2868
Ta(110)	287.9	291.6	67.8	144.9	141.2	16.65	1902
A	155.0	137.6	29.9	77.6	69.1	6.47	2060
B	179.9	155.0	34.0	88.5	77.2	8.64	1905
QPFSL	162.0	142.0	31.0	80.6	71.2	7.08	2004
Expt.	167±7		38±0.5				2210

measurements were also extended to three periodic Ta/Al systems with periods less than 100 Å. The experimental data have also shown that all of the measured c_{44} are always enhanced with an amplitude ranging from $\sim 10\%$ to $\sim 30\%$.[22] This implies that the observed enhancement in the c_{44} seems not to be associated with effects of the quasiperiodic layering on the wave propagation, and may be only relevant to the underlying physical causes.

The nature of the interface may be central to this issue. Usually, an ideal superlattice should have perfect interfaces and no fluctuations in thickness of each constituent layer. However, in practice, this is not the case for compositionally modulated materials. A large size mismatch of the two kinds of atoms may lead to a diffuse interface between Ta and Al layers. Alternatively, the large difference of the atomic masses makes the phonon spectrum sensitive to the local bonding configurations and to fluctuations in the chemical composition. Based on the previous work of Jiang *et al.*,[9] we hence modeled this by assuming that the interface extends over several monolayers with an average composition of $Ta_{0.5}Al_{0.5}$, giving rise to a partial error-function-like profile.

Using this model, we found that the effect of the diffuse interface varies for different elastic constants. The effective elastic constant c_{11} of the QPFSL's is only slightly altered by the interface broadening. This behavior can be explained by the fact that the longitudinal threshold in the phonon spectrum is determined largely by bulk-acoustic-wave propagation along the surface, so that it doesn't respond sensitively to changes at the interface. The shear elastic constant c_{44} of the basic elements is strongly affected by disorder at the interface. Figure 3 illustrates this dependence of the interface effect on the effective elastic constants c_{44} and c_{11}.

One finds from this figure that if the interface layer due to atomic diffusivity is true for the present cases, then the measured c_{44}^{expt}(QPFSL) falls into the range of c_{44}^{A} and c_{44}^{B} only when the interface width is greater than 8 Å. In particular, while the enhancement of the measured c_{44} is mainly due to the contribution of the basic element B sublattices, the estimate of the possible interface width is just accordance with Refs. 9 and 10. Although this speculation is not in good agreement with the calculated c_{44}^{cal}(QPFSL), it demonstrates the effect of interface broadening on the possibility of observing an elastic-constant enhancement.

The Brillouin cross section and phonon density of states based on the measured and calculated elastic constants, shown in Table I, have been plotted in Figs. 4(a) and 4(b) and compared with the observed phonon spectrum (dots). The data in the range 13–23 GHz have been extended so that the longitudinal threshold or dip position is clearly shown. The calculations indicate that the

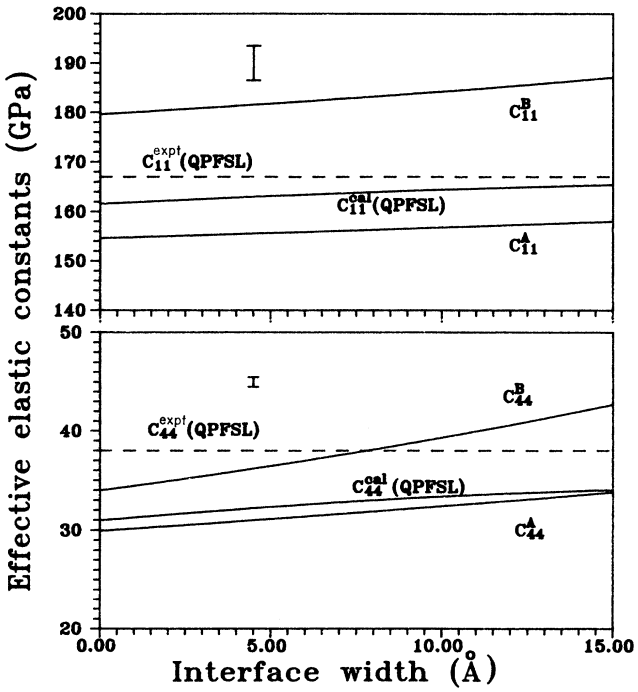

FIG. 3. Dependence of the effective elastic constants in both the two basic elements and the QPFSL's vs the interface width. In this case, the QPFSL's are modeled by Ta and Al layers separated by a disordered interfacial layer of composition $Ta_{0.5}Al_{0.5}$ because of the large difference between the atomic masses of Ta and Al. The dashed lines correspond to the measured elastic constants.

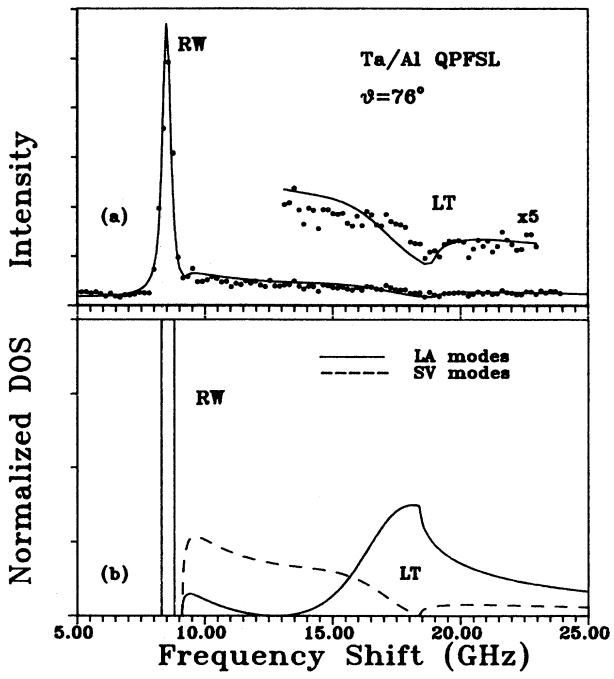

FIG. 4. (a) Comparison of the phonon spectrum observed experimentally with the calculated Brillouin cross section based on the measured elastic constants for Ta/Al QPFSL's. RW denotes the Rayleigh-wave peak, while LT indicates the dip corresponding to the longitudinal threshold. (b) Calculated normalized phonon density of states of long-wavelength phonons with a maximum peak corresponding to the longitudinal threshold.

ripple scattering process is found to account accurately for the relative intensity of our spectrum. This means that the photoelastic contribution for the modulation of the phonon spectra is not important, especially for Ta/Al QPFSL's. Here the theoretical cross section is calculated in the limit of film thickness much higher than phonon wavelength; in addition, we have convolved the theoretical cross section with a Gaussian representing the instrumental resolution function, and the intensity scale of the fitting spectrum is normalized to the height of the Rayleigh-wave peak. If detailed structures are ignored, our simulation is comparable to the observed spectrum. In Fig. 4(b) we have also plotted the phonon density of states in the Ta/Al QPFSL's with respect to longitudinal and shear-vertical phonon vibrational modes. It can be seen that the so-called "dip" position in Figs. 2 and 4(a) corresponds, in fact, to the maximum longitudinal density of states from long-wavelength bulk-acoustic phonons.

V. SUMMARY

We have investigated the effective elastic properties of quasiperiodic superlattices both theoretically and experimentally. In particular, the effective-medium approximation has been further developed for quasiperiodic structures, based on the previous work of Grimsditch and Nizzoli. The close-form effective elastic tensor obtained is very similar to that of periodic superlattices. This property, implying periodicity on a logarithmic scale, reflects the self-similarity of the Fibonacci sequence. It is also unsurprising since the long-wavelength phonons or acoustic Goldstone modes are not sensitive to microscopic detail.[23] Nevertheless, we should note that the differences between quasiperiodic and periodic results may still be striking if the difference of acoustic impedances in the two basic elements is not negligible.[7,14,20]

In this paper, surface phonon spectra from Ta/Al QPFSL's are presented with use of the Brillouin-light-scattering technique. From the measured dip position corresponding to the longitudinal threshold as well as the Rayleigh-wave velocity, we have obtained an accurate determination of c_{11} and c_{44}. A comparison of the measured c_{11} and c_{44} with those calculated demonstrates reasonable agreement for c_{11}, but an appreciable discrepancy of $\sim 20\%$ for c_{44}. This result is quite real but so far not well explained.

The effect of the presence of a diffuse interface on the elastic properties has been examined. The fitted data demonstrated that such an effect gives rise to a nonnegligible enhancement of the shear modulus. This result is important, not only for quasiperiodic superlattices, but for periodic superlattices as well. Although we could not give unambiguous evidence to argue for the effects of the quasiperiodic or periodic layering on the elastic anomalies, the large discrepancy between predicted and measured c_{44} seems to be related to elastic hardening in Ta/Al superlattices, owing to the similarity in the structure with respect to Au/Cr superlattices.[24] Indeed it should be worthwhile investigating this anomaly, but due to the lack of available samples with different modulation wavelengths these experimental studies have yet to be performed. Therefore, further theoretical and experimental studies are highly desirable.

ACKNOWLEDGMENTS

This research was supported by the National Provincial Natural Science Foundation, Science Foundation of Education Committee of China, as well as by Consorzio Interuniversitario di Fisica della Materia, Italy.

[1]R. Merlin, K. Bajema, R. Clark, R.-Y. Juang, and P. K. Bhattacharya, Phys. Rev. Lett. **55**, 1768 (1985).
[2]Xing-kui Zhang, Hua Xia, Guang-xu Cheng, An Hu, and Duan Feng, Phys. Lett. A **136**, 312 (1989).
[3]D. J. Lockwood, A H. MacDonald, G. C. Aers, M. W. C. Dharma-wardana, R. L. S. Devine, and W. T. Moore, Phys. Rev. B **36**, 9286 (1987).
[4]M. Nakayama, H. Kato, and S. Nakashima, Phys. Rev. B **36**, 3472 (1987).
[5]D. W. C. Dharma-wardana, A. H. MacDonald, D. J. Lockword, J.-M. Baribeau, and D. C. Houghton, Phys. Rev. Lett. **58**, 1761 (1987).
[6]G. C. Aers, M. W. C. Dharma-wardana, G. P. Schwartz, and J. Bevk, Phys. Rev. B **39**, 1092 (1989).
[7]Hua Xia, X. K. Zhang, G. X. Cheng, Wei Zhang, X. X. Qu, and Duan Feng, Phys. Rev. B **44**, 8779 (1991).
[8]J. R. Sandercock, in *Light Scattering in Solids III,* edited by M. Cardona and G. Güntherodt (Springer, Berlin, 1982), Vol. 51, p. 173; Solid State Commun. **26**, 547 (1978).
[9]S. S. Jiang, A. Hu, H. Chen, W. Liu, Y. X. Zhang, Y. Qiu, and D. Feng, J. Appl. Phys. **66**, 2258 (1989).
[10]R. W. Peng, A. Hu, and S. S. Jiang, Appl. Phys. Lett. **59**, 2512 (1991); S. S. Jiang, J. Zou, D. J. H. Cockayne, A. Sikorski, A. Hu, and R. W. Peng, Philos. Mag. B **66**, 229 (1992).
[11]V. Bortolani, A. M. Marvin, F. Nizzoli, and G. Santoro, J. Phys. C **16**, 1757 (1983).
[12]S. Tamura and J. P. Wolfe, Phys. Rev. B **38**, 5610 (1988).
[13]Seiji Mizuno and Shin-ichiro Tamura, Phys. Rev. B **45**, 734 (1992).
[14]Bernard Jusserand, Daniel Paquet, Francis Mollot, Marie Christine Joncour, and Bernard Etienne, Phys. Rev. B **39**, 3683 (1989).
[15]B. Jusserand, D. Paquet, F. Mollot, F. Alexandre, and G. Le Roux, Phys. Rev. B. **35**, 2808 (1987).
[16]M. Grimsditch, Phys. Rev. B **31**, 6818 (1985).
[17]M. Grimsditch and F. Nizzoli, Phys. Rev. B **33**, 5891 (1986).
[18]E. Akcakaya, G. W. Farnell, and E. L. Adler, J. Appl. Phys. **68**, 1009 (1990).
[19]A. Nougaoui and B. Djafari Rouhani, Surf. Sci. **185**, 154 (1987).
[20]Hua Xia, X. K. Zhang, K. J. Chen, G. X. Cheng, D. Feng, G. Socino, L. Palmieri, G. Carlotti, D. Fioretto, and F. Nizzoli, Phys. Rev. B **42**, 11 288 (1990).
[21]M. J. P. Musgrave, *Crystal Acoustics* (Holden Day, San Francisco, 1970), p. 177.
[22]Hua Xia, An Hu, S. S. Jiang, X. K. Zhang, G. Carlotti, D. Fioretto, and G. Socino (unpublished).
[23]F. Nori and J. P. Rodriguez, Phys. Rev. B **34**, 2207 (1986).
[24]P. Bisanti, M. B. Brodsky, G. P. Felcher, M. Grimsditch, and L. R. Sill, Phys. Rev. B **35**, 7813 (1987).